J Mater Sci (2007) 42:6404–6411
DOI 10.1007/s10853-006-1197-y

Crack propagation in layered Al_2O_3/ZrO_2 composites prepared by electrophoretic deposition

Hynek Hadraba · Jan Klimes · Karel Maca

Received: 25 January 2006 / Accepted: 31 October 2006 / Published online: 25 April 2007

Abstract Crack propagation through layered Al_2O_3/ZrO_2 composites was studied. The specimens were prepared via electrophoretic deposition of alumina and zirconia powders from suspensions with monochloroacetic acid and isopropanol. The kinetics of electrophoretic deposition could be described fully if the electrophoretic mobility and conductivity of suspensions were known. The conductivity of suspensions increased in the course of deposition. Adjusting to properly controlled kinetics of deposition and sintering, deposits were prepared with strongly bonded layers of different pre-defined thicknesses and, consequently, with different magnitudes of residual stress. Cracks, produced by an indentation technique, propagated askew towards layer interfaces deflected towards the interface in the Al_2O_3 layers and away from the interface in the ZrO_2 layers. Changes in the direction of crack propagation were described for the whole range of angles of incidence (0°–90°). The biggest change in the crack propagation was observed for the angle of incidence 45° and was ca. 15°, irrespective of the magnitude of residual stress in the layers.

H. Hadraba · J. Klimes · K. Maca (✉)
Department of Ceramics, Brno University of Technology, Technicka 2896/2, 616 69 Brno, Czech Republic
e-mail: maca@fme.vutbr.cz

Present Address:
H. Hadraba
Institute of Physics of Materials, Academy of Sciences of the Czech Republic, Zizkova 22, 616 62 Brno, Czech Republic

Introduction

Much current research into new materials is based on the desire to obtain materials with quite specific properties. In connection with this trend the so-called tailored materials or functionally gradient materials are mentioned in the literature. The term ''functionally gradient material'' refers to a heterogeneous material whose structural components are of intentionally non-uniform distribution. In such materials, a change in the composition results in a change in physical and chemical properties in a certain direction. The simplest functional gradation of material properties is on the interface of two materials of different physical properties. This happens in a range of applications, from the simplest such as surface layers up to complicated layered systems. Today much attention is paid to examining the effect of functional gradation of a material on its mechanical properties, in particular crack propagation through a layer interface.

Two basic types of layered ceramics are described in the literature: composites with weakly bonded layers [1] and composites with strongly bonded layers [2]. The physical mechanisms of the transfer of stress across the layer interface are different in the two types of composite, and so are also the mechanisms of crack propagation through the layer interface. In composites with weakly bonded layers the deflection of a propagating crack on the interface of two materials and multistage fracture in bending can be observed; these lead to increased fracture toughness of composites, accompanied by a decrease in their strength and integrity. This prevents their use in structural applications. In composites with strongly bonded layers, however, the deflection or bifurcation of crack propagation occurs when the extending crack passes through the interface of two materials. This mechanism also causes an

increase in fracture toughness but this time without any decrease in the other mechanical properties. The above deflection and bifurcation are usually explained by the existence of residual stress in the interface of two phases and by the mismatch of the elastic properties of the two bonded materials.

One of the methods used to prepare layered material with strongly bonded layers is electrophoretic deposition [2–5]. If the kinetics of electrophoretic deposition is carefully adjusted, the thickness of layers in the composite can be controlled and, at the same time, high final relative densities and strong bonding of layers can be obtained [4]. Fracture behaviour of composite materials with strongly bonded layers (prepared by electrophoretic deposition) was the subject of studies, for example, by Hatton and Nicholson [2, 3] and Hadraba et al. [4]. When propagating through the Al_2O_3/ZrO_2 interface, a crack deflected in the ZrO_2 layer away from the interface, and in the Al_2O_3 layer towards the interface of these layers. Prakash et al. [2] related this behaviour to the presence of thermal stress arising in the composite because of the different properties (different initial relative densities of Al_2O_3 and ZrO_2 deposits) and physical behaviour (different coefficients of thermal expansion of Al_2O_3 and ZrO_2). The magnitude of tensile stress in the ZrO_2 layer can be calculated according to the relation (1) presented by Hillmann et al. [6]:

$$\sigma_{rZrO_2} = \frac{(CTE_{ZrO_2} - CTE_{Al_2O_3}) \cdot \Delta T \cdot E_{ZrO_2}}{1 - v_{ZrO_2}} \cdot \left(1 + \frac{\bar{t}_{ZrO_2}}{\bar{t}_{Al_2O_3}} \cdot \frac{E_{ZrO_2}/(1 - v_{ZrO_2})}{E_{Al_2O_3}/(1 - v_{Al_2O_3})}\right)^{-1}, \quad (1)$$

where $\bar{t}\,(\mu m)$ is the average layer thickness, CTE (K^{-1}) is the coefficient of linear thermal expansion, ΔT(°C) is the difference between the sintering and the current temperature, v(–) is Poisson's ratio, and E (MPa) is the modulus of elasticity. Stress in the Al_2O_3 ($\sigma_{Al_2O_3}$) phase can be obtained by interchanging the indices of quantities. The directions of the compression (Al_2O_3) and tensile (ZrO_2) residual thermal stresses in layers are parallel to the layer interface.

In the tensile stress field of the ZrO_2 layer the crack deflects away from the layers because its propagation is made easier due to its opening out in the tension field. After passing through the interface, the crack in the Al_2O_3 layer deflects towards the layer interface in order to propagate in parallel to the compressive stress in this layer. Oechsner [7] suggested that the bifurcation of crack path in strongly bonded laminates is caused mainly by the presence of residual stresses in layers, but also the mismatch of elastic moduli and fracture toughness of bonded materials plays a significant role. Oechsner studied extension of macroscopic cracks in specimens subjected to four-point bending. The role of these two contributions has not been clearly explained in the case of deflection of surface indentation cracks.

It is obvious from Eq. 1 that, by merely changing the ratio of the Al_2O_3 and ZrO_2 thicknesses, a composite with a different magnitude of residual stresses in the layers can be prepared. Since these stresses are thought to be responsible for the deflection in the direction of crack propagation, perfect control of the process of applying a layer of defined thickness is an important element in the preparation of layered composites with desired properties. In the case of electrophoretic deposition this involves an exact description of deposition kinetics.

These kinetics have been described by Zhang et al. [8], who derived a relation for the deposited mass (m) as a function of deposition time (t) during electrophoretic deposition in the constant-current mode:

$$m(t) = m_0\left(1 - e^{-\frac{\mu \cdot U}{d^2}t}\right), \quad (2)$$

where m_0 (kg) is the initial mass of particles in the suspension, d (m) is the distance between electrodes, U (V) is electric voltage, μ ($m^2\ V^{-1}$) is the electrophoretic mobility of particles, and t (s) is the time of deposition. Maca et al. [9] studied the kinetics of electrophoretic deposition of Al_2O_3 in a medium containing isopropanol and monochloroacetic acid. They fitted the dependence of deposit thickness h (m) on time t (s) to the following equation, which is based on that of Zhang cited above:

$$h(t) = \frac{100 \cdot m_0}{S \cdot \rho_{theor} \cdot \rho_{rel-g}}\left(1 - e^{-\frac{\mu \cdot U}{d^2} \cdot t}\right), \quad (3)$$

where S (m^2) is the electrode surface, ρ_{theor} (kg m^{-3}) is the theoretical density of the ceramic under study, and $\rho_{rel\text{-}g}$ (%) is the relative density of deposit subsequent to annealing. They found that, for a non-sedimenting (stable) suspension, Eq. 3 fitted well the growth of deposit thickness with time, but the values m_0 or μ calculated from regression coefficients differed slightly from the actual amount of Al_2O_3 powder in the suspension or from the electrophoretic mobility measured with a Zetasizer.

One of the aims of the present work was to provide a more exact model of the kinetics of electrophoretic deposition such that the thickness of the deposited layers could be predicted reliably, and then to prepare layered ceramic composites Al_2O_3/ZrO_2 of different layer thicknesses. Another aim was to describe the propagation of indentation cracks through alumina/zirconia and zirconia/alumina interfaces and consider the effect of different magnitudes of residual stress in layers on indentation crack deflection.

Experimental

Materials

For the preparation of composites, Al_2O_3 powder (type RC-HP-DBM, Malakoff Ind., USA) with a mean particle size of 470 nm and ZrO_2 stabilized with 3 mol% of Y_2O_3 (type TZ-3YSE, Tosoh, Japan) with a mean particle size of 140 nm were used.

The dispersion medium used in the preparation of suspensions of Al_2O_3 and ZrO_2 powders was isopropanol (p.a., Onex, Czech Republic). Monochloroacetic acid (99%, Aldrich, Germany) was added to the suspensions to aid stabilization and dispersion. The amount of water in the ceramic powders was reduced to a minimum via drying at 100 °C for 40 min.

Electrophoretic deposition

The suspensions used for electrophoretic deposition were prepared by mixing 15 wt.% of Al_2O_3 or ZrO_2 powder with 85 wt.% of liquid phase (12.75 wt.% monochloroacetic acid in 72.25 wt.% isopropanol). This composition was established as optimum for electrophoretic deposition of these ceramic powders in previous work [9].

Electrophoretic deposition was performed in a horizontal electrophoretic cell with two graphite electrodes. The electrode distance d was 26 mm and the effective electrode surface S (the surface actually immersed in the suspension) was 18.7 cm^2. The cell design (see Fig. 1) made it practically impossible for any of the suspension to flow into the space behind the electrodes. The voltage output from the source into the cell was registered by a linear two-channel recorder via a measuring transformer (Fig. 1).

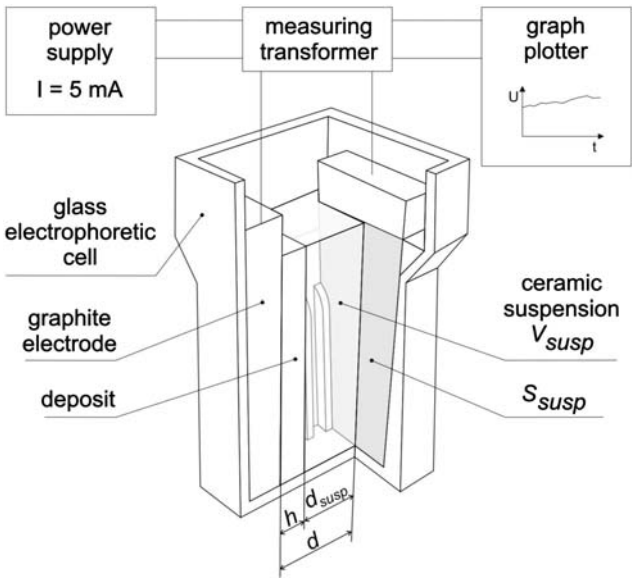

Fig. 1 Cell cross-section and schematic of instrument connection in electrophoretic deposition

Electrophoretic deposition proceeded in constant current mode at 5 mA. The source of constant current was a microcomputer-controlled stabilized source of dc voltage (E815, Consort, Belgium). In order to prevent particles from sedimenting the suspension was stirred repeatedly during electrophoretic deposition. In the case of single-phase deposit the deposition was interrupted every 5 min, the electrodes were briefly removed and the suspension was stirred. At the same time, a micrometre slide gauge was used to measure the thickness of deposited layer at three vertical levels: 18, 38, and 58 mm from the top of the suspension.

Two-phase layered composites were prepared by 59 consecutive deposition steps alternatively in Al_2O_3 and ZrO_2 suspensions. In this case the suspensions were stirred after the deposition of every single layer, i.e. after a period of 8–72 s for Al_2O_3, and 47–183 s for ZrO_2 (depending on the layer thickness). During the deposition, the specific electric conductivity of the suspension was measured using a conductometer (Accumet, Denver Instrument Comp., USA).

Table 1 gives the planned thickness ratios of individual layers of layered composite materials. Each composite deposit consisted of 30 Al_2O_3 and 29 ZrO_2 alternating layers.

Treatment of deposits

The moist deposit was first dried on the electrode for a period of 3 h at room temperature. During drying, all the samples cracked into a few pieces which, however, were still large enough for further treatment. They were removed from the electrode and dried for another 12 h under the same conditions. Subsequently, the deposit was annealed (800°C/1 h; heating rate + 2 °C/min) and sintered (1500 °C/2 h; heating rate + 2 °C/min) in air.

Table 1 Layer thickness ratios of prepared layered composite materials

Designation	Phase composition	Thickness ratio $\bar{t}$ of Al_2O_3:ZrO_2 layer
Al3/Zr1	Al_2O_3/ZrO_2	3:1
Al2/Zr1	Al_2O_3/ZrO_2	2:1
Al1/Zr1	Al_2O_3/ZrO_2	1:1
Al1/Zr2	Al_2O_3/ZrO_2	1:2
Al1/Zr3.5	Al_2O_3/ZrO_2	1:3.5
Al1/Zr10	Al_2O_3/ZrO_2	1:10

Evaluation of deposit properties

The density of the deposit was determined using Archimedes' method (EN 623-2). Polished specimens of sintered deposits were prepared by standard ceramographic methods. The microstructure of deposits was observed by means of scanning electron microscopy (XL 30, Philips, the Netherlands).

Cracks were produced in the polished specimens using a Vickers indentor (hardness tester Wolpert diatestor 2Rc, Germany). Indentations were performed at a loading force of 98 N with a holding time of ca. 10 s. The distance between indentations was ca. five times the length of the indentor diagonal. About 55 indentations were made on each specimen.

Pictures of indentation cracks were taken on an optical microscope (GX71 Olympus, Japan). The angles by which crack propagation is described were measured via image analysis using the Atlas software (Tescan, Czech Republic).

Results and discussion

Kinetics of electrophoretic deposition

Figure 2 gives the measured and calculated dependence of layer thickness on deposition time for the Al_2O_3 suspension. The full line was constructed by Eq. 3, substituting the values: $m_0 = 11.6$ g, d = 26 mm, $S = 18.7$ cm^2, $\rho_{theor} = 3.99$ g cm^{-3}, $\rho_{rel\text{-}g} = 60\%$, $U = 109.2$ V, and $\mu = 0.275$ μm cm V^{-1} s^{-1}, which is the electrophoretic mobility of this suspension measured with a Zetasizer [9]. As can be seen from Fig. 2, the experimentally measured thickness values of layers were lower than predicted by model Eq. 3. In [9] a similar experimental dependence was fitted with a regression function, and from its comparison with model Eq. 3 the values $m_0 = 10$ g and $\mu = 0.475$ μm cm V^{-1} s^{-1} were calculated. The deflections of these values from the experimental data were explained by the authors claiming that part of the suspension during deposition was behind the electrodes and the measurement of electrophoretic deposition was carried out on a suspension with lower particle concentration.

In our experiment the possible effect of the suspension running behind the electrodes was eliminated by using electrodes of a suitable shape (Fig. 1). To explain the remaining deviation of theory and experiment the voltage on the electrodes was measured in the present work in the course of the whole experiment. As can be seen from Fig. 3, a voltage drop was recorded during deposition. In [9] the voltage was not measured during deposition and so in the calculation of the dependence of layer thickness on time the electric voltage was considered to be constant. If, in Eq. 3, we substitute the experimentally found time dependence of voltage $U(t)$ (Fig. 3), we have a very good agreement of the theoretical model of growth kinetics of deposited Al_2O_3 layer with experimentally measured data (see Fig. 4). In view of this good agreement it is obvious that electrophoretic mobility of Al_2O_3 in the suspension used was $\mu = 0.275\ \mu m\,cm\,V^{-1}\,s^{-1}$. This value was thus confirmed both by the measurement of growth kinetics of deposited layer and by separate measurement on a Zetasizer [9].

In the next section we will try to explain the drop in electric voltage in the course of deposition. Since the experiments proceeded at constant current $I = 5$ mA, it follows from Ohm's law that during deposition the electric resistance R (Ω) was decreasing. At the beginning of deposition the electrical resistance of the system was only given by the suspension resistance R_{susp} (Ω). In the course of the experiment the ceramic layer on the anode is

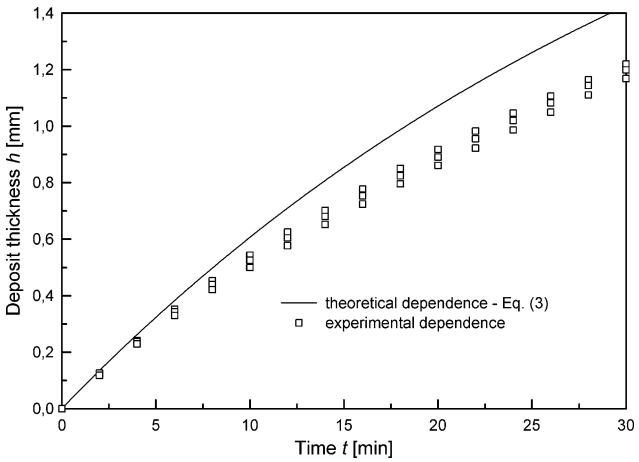

Fig. 2 Dependence of layer thickness on deposition time

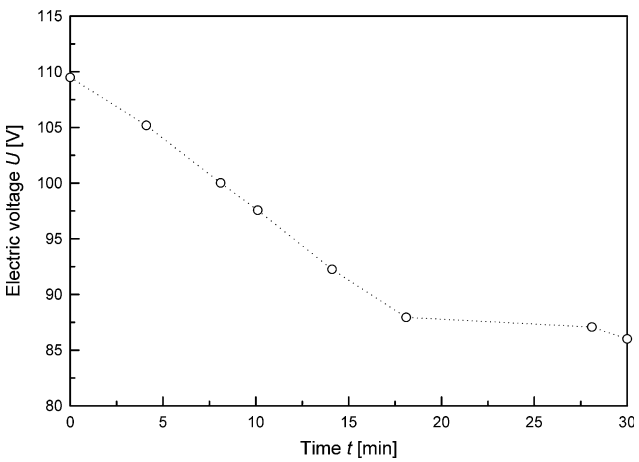

Fig. 3 Dependence of electric voltage on deposition time

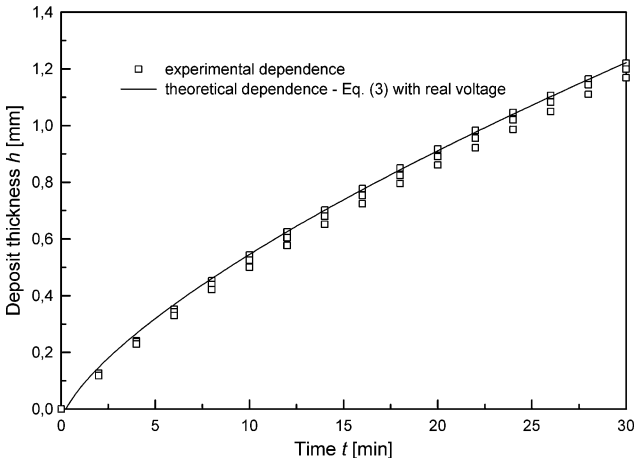

Fig. 4 Dependence of experimentally established and theoretical layer thicknesses on deposition time (with the actual electric voltage included)

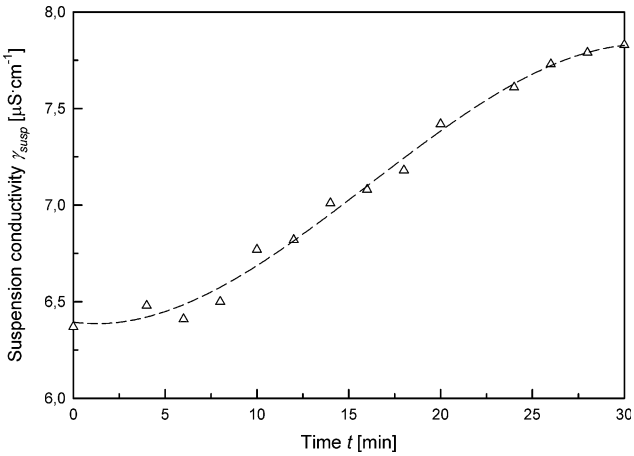

Fig. 5 Dependence of suspension conductivity on deposition time

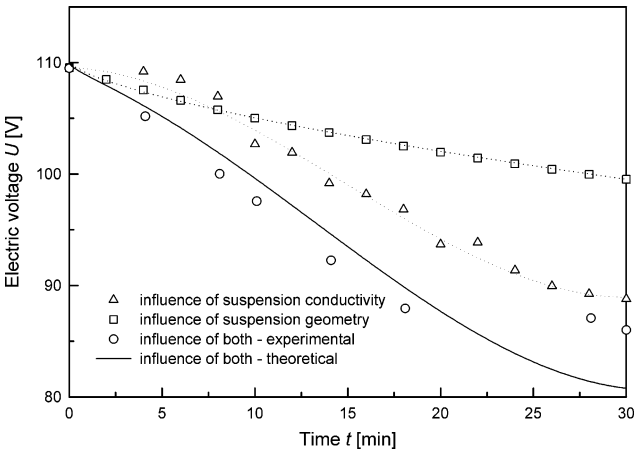

Fig. 6 Dependence of electric voltage on deposition time, with the effect of geometry and suspension conductivity included

growing, and the total resistance of the system R is given by the sum of the resistance of suspension R_{susp} and the resistance of the deposited layer R_{layer} (Ω). Since the system's total resistance R was decreasing, we will consider a variant in which the resistance of deposited layer R_{layer} is negligible (either because of its small thickness or because of the high conductivity due to the liquid phase contained in the pores of the layer). The drop in total resistance is thus caused by the change in resistance of the suspension. The electrical resistance of the suspension is given by the relation:

$$R_{\text{susp}} = \frac{1}{\gamma_{\text{susp}}} \cdot \frac{d_{\text{susp}}}{S_{\text{susp}}}, \tag{4}$$

where γ_{susp} (S m^{-1}) is the conductivity of the suspension, d_{susp} (m) and S_{susp} (m^2) describe the experimental arrangement (see Fig. 1). All these quantities could contribute to the decrease of R_{susp}.

Measurements during the experiment showed an increase in the conductivity of the suspension (Fig. 5). The cause of this phenomenon is unknown: it could be due, for example, to increased dissociation of monochloroacetic acid, caused probably by the change of suspension composition, or by the action of electric field. But the increase itself in the conductivity of suspension cannot explain the actual drop in electric voltage fully (see Fig. 6). To do so, it would be necessary to take into consideration the other phenomena observed during deposition—for example, the geometry change of the liquid phase.

The quantities d_{susp} (m) and S_{susp} (m^2) (see Fig. 1) in Eq. 4 are at the beginning of the experiment of the same value as d and S in Eq. 3. The distance d_{susp}, however, decreases during deposition by the thickness of deposited layer given by Eq. 3. Assuming that the volume of suspension remains constant ($V_{\text{susp}} = 48.62$ cm^3) during experiment (i.e. neglecting the effects of isopropanol evaporation and particle deposition), the electrode surface S_{susp} increases owing to the increased height of suspension due to the deposit growing on the electrode. The temporal change of the $d_{\text{susp}}/S_{\text{susp}}$ ratio will thus be given by the relation:

$$\frac{d_{\text{susp}}}{S_{\text{susp}}} = \frac{d - h(t)}{\frac{V_{\text{susp}}}{d_{\text{susp}}}} = \frac{d - h(t)}{\frac{V_{\text{susp}}}{d - h(t)}} = \frac{(d - h(t))^2}{V_{\text{susp}}}, \tag{5}$$

where $h(t)$ (mm) is the time dependence of layer thickness given by the Eq. 3. The possible effect of the change in electric resistance of suspension (caused by the change in suspension geometry) on electric voltage in the course of deposition is illustrated in Fig. 6.

To explain the drop in the resistivity of the suspension it was necessary to take into account the above two phe-

nomena together—the increase in the suspension conductivity and the geometry change of the liquid phase (see Fig. 6). The increase in suspension conductivity was the more significant of these two phenomena. A relatively large deviation of measured values of electric voltage from the given theoretical calculation was observed at longer deposition times. This could mean that, after a certain period of time, some effects causing decelerating of electric resistance drop take place (e.g. decrease of S_{susp} due to suspension evaporation,...).

It follows from the above findings that electrophoretic deposition in the constant-current mode is in agreement with the theoretical relation derived by Zhang et al. [8]. The growth rate of the layer being deposited can be predicted knowing the electrophoretic mobility of the particles and the specific suspension conductivity.

Structure and properties of layered deposits

Apart from properly controlling the kinetics of electrophoretic deposition it is necessary, when preparing layered deposits with exactly defined thicknesses of individual layers, to consider also the different sintering kinetics of individual materials. In our case, the green density $\rho_{rel\text{-}g}$ of Al_2O_3 and ZrO_2 layers was 60% and 40%, respectively, which resulted in different shrinkages during sintering. These differences in sintering could lead to the appearance of so-called sintering stresses. Although these sintering stresses are not very large [10], they might lead to the appearance of cracks or cavities on layer interfaces. Such microdefects can then have a influence on the strength of layer bonds and, ultimately, they can affect the mechanical properties of composites. As can be seen from Fig. 7 the interface of the Al_2O_3/ZrO_2 layers in the composites we had prepared did not contain any pronounced defects and the layers were properly sintered. The final relative density of layered composites was higher than 99.4%. From Table 2 it is also evident that electrophoretic deposition and sintering were controlled to such a degree that the planned ratio of the thicknesses of individual layers was achieved almost exactly (see also Table 1), and Fig. 7 documents good uniformity of the layers.

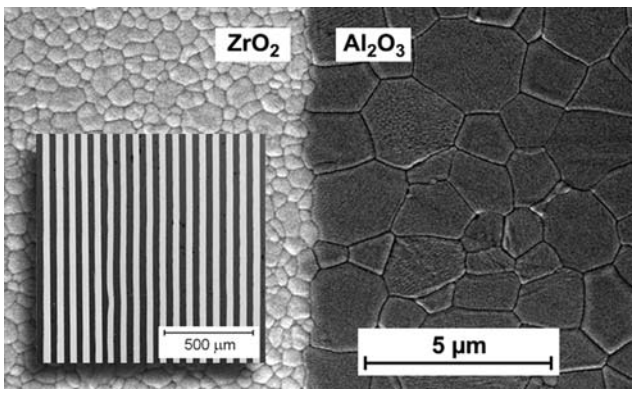

Fig. 7 Microphotograph of the interface of layered Al_2O_3/ZrO_2 composite

Table 2 Relative densities of prepared layered composite materials

Designation	Layer thickness $\bar{t}$ (μm)		Final density $\rho_{rel\text{-}f}$ (%)
	Al_2O_3	ZrO_2	
Al3/Zr1	40.0	13.0	99.93
Al2/Zr1	36.3	18.0	99.72
Al1/Zr1	43.0	43.0	99.78
Al1/Zr2	21.6	43.4	99.66
Al1/Zr3.5	12.7	46.4	99.45
Al1/Zr10	5.0	50.0	

Of greater importance than the appearance of sintering stresses in the composite is, however, the appearance of the so-called cooling stresses, i.e. residual stresses due to the different coefficients of linear thermal expansion of the two phases in the composite. The appearance of these stresses and the establishment of their magnitudes are described in detail in the theoretical part of the present work.

Table 3 gives the values of Poisson's ratio ν, elasticity modulus E, and coefficient of linear thermal expansion CTE employed in the calculation of stresses in the composites prepared.

Table 4 gives the magnitudes of residual stress in Al_2O_3 and ZrO_2 layers calculated according to Eq. 1 and with the aid of the material constants given in Table 3.

Table 3 Material constants used in the calculation of residual stress

Quantity	Al_2O_3	ZrO_2
Poisson's ratio ν (–)	0.26	0.31
Modulus of elasticity E (GPa)	380	210
Coefficient of thermal expansion CTE (K^{-1})	9×10^{-6}	10.3×10^{-6}
Theoretical density ρ_{theor} (g cm^{-3})	3.99	6.08

Table 4 Calculated magnitudes of residual stresses

Designation	Layer thickness $\bar{t}$ (μm)		Calculated residual stress σ_r (MPa)	
	Al_2O_3	ZrO_2	Al_2O_3	ZrO_2
Al3/Zr1	40.0	13.0	–159.6	+491.0
Al2/Zr1	36.3	18.0	–224.2	+452.7
Al1/Zr1	43.0	43.0	–367.7	+367.7
Al1/Zr2	21.6	43.4	–537.4	+267.1
Al1/Zr3.5	12.7	46.4	–675.9	+185.0
Al1/Zr10	5.0	50.0	–845.4	+84.5

Sign convention: + = tension, – = compression

It follows from the above findings that, using electrophoretic deposition, it is possible to prepare layered composite materials with strongly bonded layers. The interface between layers was properly sintered and there was no increased concentration of microstructural defects on the interface or in its neighbourhood. According to the calculations performed, there were residual compression stresses from 160 to 845 MPa in the Al_2O_3 layers, and residual tensile stresses from 85 to 490 MPa in the ZrO_2 layers.

Crack propagation through layer interface

To study crack propagation through layer interfaces the cracks propagating from the corners of the Vickers indentor (the so-called indentation cracks) were used. The indentor orientation was chosen such that the cracks propagated to the interface at different angles (see Fig. 8). On each of the five composites, ca. 50 indentations with four cracks were performed, i.e. a total of ca. 1,000 measurements.

Angle α, at which the crack reached the interface of layers will be called the angle of incidence, while angle β, at which the crack refracted after passing through the interface will be called the angle of refraction (see Fig. 8). The change in crack propagation direction is designated as $\Delta\alpha$ in Fig. 8:

$$\Delta\alpha = \beta - \alpha. \tag{6}$$

It can be seen from Fig. 8 that $\Delta\alpha$ is negative for crack propagation from Al_2O_3 to ZrO_2($\beta_{AZ} < \alpha_{AZ}$, $\Delta\alpha_{AZ} < 0$) and positive for crack propagation from ZrO_2 to Al_2O_3($\Delta\alpha_{ZA} > 0$).

The dependence of the angle of refraction β on the angle of incidence α (including the 95% confidence interval), irrespective of the magnitude of residual stress in the layers, is shown in Fig. 9. There it can be seen that the biggest change in crack propagation direction was observed for the angle of incidence of about 45°:$\Delta\alpha_{ZA}$ = + 15°, $\Delta\alpha_{AZ}$ = –15°. On the other hand, and in accordance with the

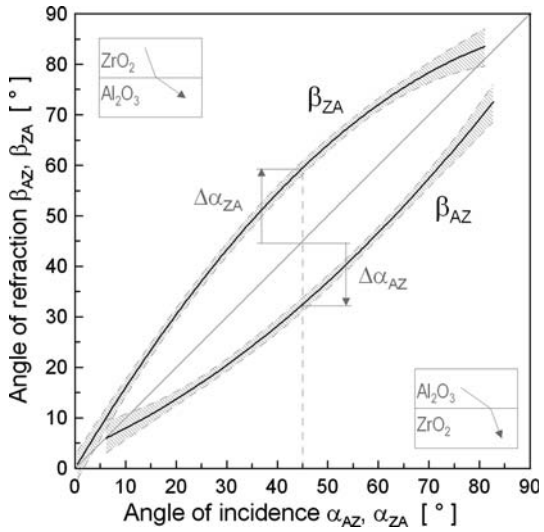

Fig. 9 Dependence of deflection angle on incidence angle of a crack propagating through interface in composites

previous work [4], the cracks propagating nearly parallel to the interface ($\alpha \rightarrow 90°$) as well as cracks propagating normally (perpendicularly) to the interface ($\alpha \rightarrow 0°$) were not deflected at the interface and thus a change in crack propagation was not observed.

The behaviour of the crack passing through the width of the whole layer can be seen in Fig. 10. The crack propagating from alumina to zirconia and again to alumina was propagating again in the same direction, but its trajectory was shifted. It is was found that the angle in which the crack approached alumina/zirconia interface and angle in which it left the zirconia/alumina interface were equivalent

$$\alpha_{AZ} = \beta_{ZA} \tag{7}$$

Resulting from geometrical analysis of the Fig. 10, the magnitude of the crack shift depends on $\Delta\alpha$ and on layer thickness and the change in crack propagation $\Delta\alpha_{AZ}$ and $\Delta\alpha_{ZA}$ are of the same magnitude but opposite sign:

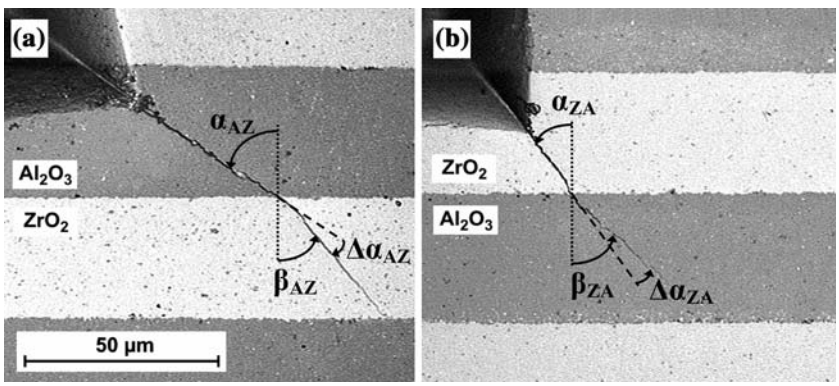

Fig. 8 Indentation cracks propagating askew to the layer interface in layered Al1/Zrl composite (**a**) from Al_2O_3 into ZrO_2 (**b**) from ZrO_2 into Al_2O_3

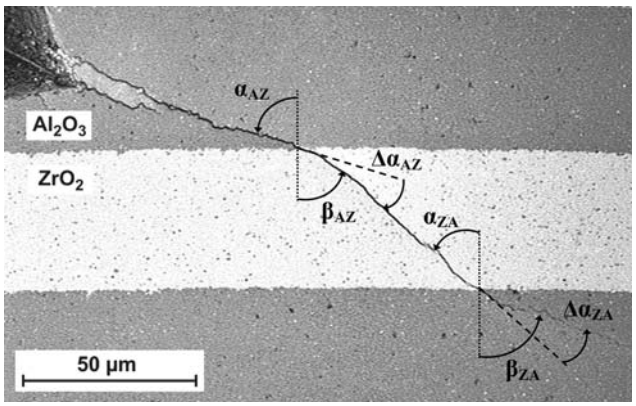

Fig. 10 Parallel shifting of a crack propagating through the whole thickness of one layer

$$\Delta\alpha_{AZ} = -\Delta\alpha_{ZA}. \quad (8)$$

The observations described by Eqs. 7 and 8 explain the symmetry of the experimentally obtained values of β_{AZ} and β_{ZA} along the $\beta = \alpha$ graph diagonal.

In the composites we prepared, the magnitude of residual stresses changed in the range from +491 to +84.5 MPa for ZrO_2 and from –845.4 to –159.6 MPa for Al_2O_3. The dependence of the change in crack propagation $\Delta\alpha$ for the angle of incidence $\alpha = 45°$ on the magnitude of residual stresses is shown in Fig. 11. The figure includes the 95% confidence interval acquired by analysis of the measured data with reference to the magnitude of residual stress in the layers. It is evident from the figure that, within experimental error, the deflection of crack propagation did not depend on the magnitude of introduced tensile (ZrO_2) and compression (Al_2O_3) residual stresses.

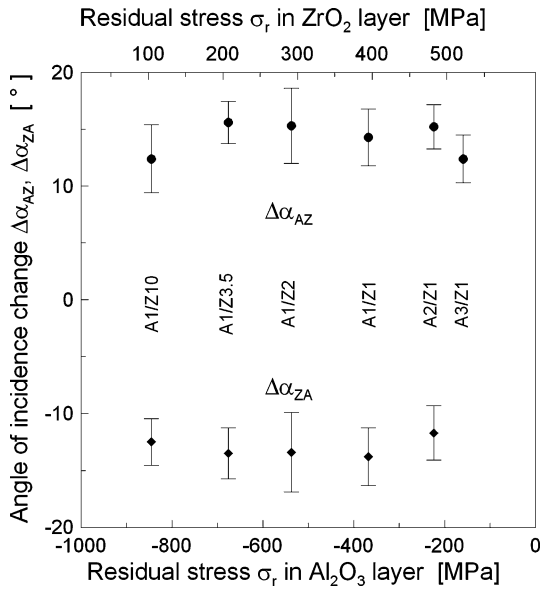

Fig. 11 Dependence of incidence angle difference on the magnitudes of residual stresses in composite layers (angle of incidence $\alpha = 45°$)

Conclusion

The subject of study was electrophoretic deposition of Al_2O_3 and ZrO_2 layers deposited from suspensions with monochloroacetic acid and isopropanol in the constant electric current mode. The kinetics of electrophoretic deposition corresponded to Zhang's theoretical model, with the mobility of electrophoretic particles corresponding to the value established by measuring the zeta potential. In the course of electrophoretic deposition the conductivity of the suspension applied increased.

Alternating electrophoretic deposition of Al_2O_3 and ZrO_2 resulted in the preparation of two-phase layered composite materials of high density (>99% t.d.) and strongly bonded layers. Layer thicknesses were chosen such that different theoretical residual stresses were obtained in the layers. It was found that a crack (produced in the samples by an indentation technique) propagating from Al_2O_3 into ZrO_2 deflected from its trajectory away from the layer interface (or to the interface if the crack propagated from ZrO_2 into Al_2O_3), irrespective of the magnitude of calculated residual stresses in the layers. Changes in the direction of crack propagation were described for the whole range of angles of incidence 0°–90°. The biggest change in the crack propagation was observed for the angle of incidence 45° and was ca 15°, irrespective of the magnitude of residual stress in the layers.

Acknowledgements This work was supported by the Czech Ministry of Education, project No. MSM0021630508.

References

1. Clegg WJ, Kendall K, Alford N, Button T, Birchall J (1990) Nature 347:455
2. Prakash O, Sarkar P, Nicholson PS (1995) J Am Ceram Soc 78:1125
3. Hatton B, Nicholson PS (2001) J Am Ceram Soc 84:571
4. Hadraba H, Maca K, Cihlar J (2004) Ceram Int 30:853
5. Sarkar P, Haung X, Nicholson PS (1992) J Am Ceram Soc 75:2907
6. Hillmann C, Suo Z, Lange FF (1996) J Am Ceram Soc 79:2117
7. Oechsner M, Hillman C, Lange FF (1996) J Am Ceram Soc 79:1834
8. Zhang Z, Huang Y, Jiang Z (1989) J Am Ceram Soc 72:810
9. Maca K, Hadraba H, Cihlar J (2004) Ceram Int 30:843
10. Cai P, Green J, Messing G (1997) J Am Ceram Soc 80:1940